Ali *et al. Virology Journal* (2025) 22:124
https://doi.org/10.1186/s12985-025-02744-4

Virology Journal

RESEARCH Open Access

Inhibition of ALKBH5 demethylase of m^{6}A pathway potentiates HIV-1 reactivation from latency

Haider Ali[1,2], Jakub Wadas[1,2], Maryam Bendoumou[3], Heng-Chang Chen[4,5], Paolo Maiuri[6], Antoine Dutilleul[3], Simona Selberg[7], Lorena Nestola[3], Kamil Lalik[1], Veronique Avettand-Fenoël[8,9], Coca Necsoi[10], Alessandro Marcello[11], Esko Kankuri[12], Mati Karelson[7], Stéphane De Wit[10], Krzysztof Pyrc[13], Alexander O. Pasternak[14], Carine Van Lint[3] and Anna Kula-Pacurar[1*]

Abstract

Background Current latency-reversing agents (LRAs) employed in the "shock-and-kill" strategy primarily focus on relieving epigenetic and transcriptional blocks to reactivate the latent HIV-1. However, their clinical efficacy is limited, partly due to their inability to fully reverse latency and the lack of LRAs specifically targeting post-transcriptional mechanisms. N6-methyladenosine (m^{6}A) modification in HIV-1 RNA is emerging as an important post-transcriptional regulator of HIV-1 gene expression, yet its role in latency and reactivation remains largely unrecognized. Here, we explored the potential of small chemical compounds targeting the m^{6}A pathway, specifically investigating the inhibition of ALKBH5 and its effect on latent HIV-1 reactivation mediated by the LRA romidepsin.

Methods We used four in vitro cellular models of latency, primary model of CD4$^+$ T cells HIV-1 infection and ex vivo cultures of CD8$^+$-depleted PMBCs from ART-treated HIV$^+$ patients. We measured latent viral reactivation by evaluating the expression of reporter protein GFP by flow cytometry, viral production by CA-p24 ELISA, and viral transcripts by RT-qPCR. CRISPR/Cas9 method was used to deplete ALKBH5. MeRIP and immuno-RNA FISH were used to address the m^{6}A methylation levels on HIV-1 RNA upon ALKBH5 inhibition.

Results We showed that ALKBH5 inhibitor 3 (ALKi-3) potentiated romidepsin-mediated viral reactivation in in vitro models of latency, primary model of CD4$^+$ T cells infected with HIV-1 as well as in ex vivo cultures of CD8$^+$-depleted PBMCs from ART-treated HIV$^+$ patients. CRISPR/Cas9-mediated depletion of ALKBH5 mimicked the effects of ALKi-3. ALKi-3 increased levels of m^{6}A-methylated HIV-1 RNA as shown by meRIP and immuno-RNA FISH.

Conclusion Our study provides a proof-of-concept for the modulation of the m^{6}A pathway in enhancing HIV-1 reactivation. This approach represents a promising adjunct to existing reactivation protocols and provides a concept of "dual-kick", aiming to target transcriptional and post-transcriptional steps in HIV-1 reactivation from latency.

Keywords HIV-1, Latency, Post-transcriptional mechanisms, Epitranscriptomics, m^{6}A, ALKBH5, Shock-and-kill, Dual-kick

*Correspondence:
Anna Kula-Pacurar
anna.kula-pacurar@uj.edu.pl

Full list of author information is available at the end of the article

Background

Antiretroviral therapy (ART) that controls Human Immunodeficiency Virus type 1 (HIV-1) infection is not curative due to the persistence of latent viral reservoir [1–4]. The "shock-and-kill" strategy is a well-established approach to reactivating latent proviruses using latency-reversing agents (LRAs). In this approach, reactivated provirus-infected cells are targeted for elimination either by the immune system or through the cytopathic effects of viral proteins, while ART is maintained to prevent new infections [5, 6]. A wide range of LRAs that activate HIV-1 transcription have been identified and classified based on their pharmacological targets. These include (i) epigenetic drugs targeting histone deacetylases (HDAC inhibitors) and DNA methyltransferases (DNMT inhibitors), (ii) protein kinase C (PKC) agonists inducing transcription factor NF-κB, (iii) Bromodomain and Extra-Terminal domain inhibitors (BETi) inducing P-TEFb as well as (iv) immuno-modulatory LRAs including cytokines, TLR agonists and immune checkpoint (IC) inhibitors [7–9]. Clinical interventions based on individual LRA treatments failed to achieve significant reduction in the latent reservoir size, despite increases in both plasma and cell-associated viral RNA levels [10–13]. This is, at least partially, due to inefficient LRAs-mediated viral reactivation from latency in vivo and to the impaired capacity of cytolytic immune effector cells to eliminate the reservoir [14, 15].

Combinations of various LRAs simultaneously targeting distinct mechanisms of viral latency have proven to be more effective in viral reactivation. For example, combinations of PKC agonist bryostatin either with HDAC inhibitors (such as romidepsin) or with P-TEFb releasing agents (such as JQ1) synergistically caused higher viral reactivation compared with the treatment by single LRAs in lymphocytic and monocytic cellular model of viral latency, as well as in the $CD8^+$-depleted PBMCs from HIV-1 infected aviremic people living with HIV (PLWH) [16, 17]. Another example is given by the combination of histone methyltransferase inhibitors (HMTI) with either HDAC inhibitors or NF-κB inducers that exhibited higher viral reactivation than individual treatments [18]. Overall, combining different LRAs targeting diverse mechanisms of viral latency may achieve better reactivation of latent proviruses in in vitro and ex vivo models of viral latency. However, no clinical success with HIV-1 latency reversal strategies has been achieved so far indicating the need for new and more effective LRAs and their combinations. The inefficiency of LRAs may be attributed to their inability to release efficiently repressive mechanisms, as they mainly target transcriptional and epigenetic blocks and do not relieve post-transcriptional blocks [19, 20].

A major post-transcriptional RNA process is a covalent modification of RNA, which is regulated by three protein complexes: (i) "writers" that transfer a chemical group to a target position on an RNA molecule; (ii) "readers" that specifically recognize the modified nucleotide and (iii) "erasers" that remove specific chemical groups from the modified nucleotide [21]. RNA modification is a post-transcriptional mechanism that affects splicing, RNA stability, export, and translation [22, 23]. The m^6A modification on mRNA is the most prevalent modification mediated by the "writer" methyltransferases complex including METTL3, METTL14, WTAP, and KIAA1429 and "erasers" including ALKBH5 and FTO. ALKBH5 has been reported to be an important drug target for its role in various physiological processes [24–26]. By now, m^6A modification has been found on almost all types of RNA. The m^6A RNA modification plays an essential role in both physiological and pathological conditions, especially in the initiation and progression of different types of cancers [27].

The m^6A modification on HIV-1 RNA is known to positively regulate viral replication [28–30]. More specifically, silencing of METTL3/14 "writers" complex decreases the viral protein production; on the other hand, silencing of ALKBH5 "eraser" increases the viral protein production [28, 29]. The m^6A methylation regulates different steps of HIV-1 RNA biogenesis including stability, alternative splicing and nuclear export [31–34]. Interestingly, recent finding supports the role of "reader" YTHDF3 as a restriction factor [35].

Given such rapidly developing evidence of the epitranscriptomic role on physiological and pathological conditions, chemists have developed small compounds that target different component of m^6A pathway [36, 37]. Interestingly, first-in-class METTL3 inhibitors (STM2457 and STC-15) are tested currently in preclinical studies for their role in myeloid leukemia therapy, anti-coronavirus drugs, and solid tumor therapy [38–40]. Moreover, another epitranscriptomic compound, 3-deazaadenosine (DAA), has been reported to inhibit the replication of a range of viruses including RSV, IAV, and HIV-1 by inhibiting m^6A addition to viral RNAs [41–43].

In this work, we investigated the impact of previously published epitranscriptomic small chemical compounds on latent viral reactivation. These compounds target the "writer" METTL3-METTL14-WTAP complex, and "eraser" proteins FTO and ALKBH5 [36, 37, 44]. We evaluated their reactivation potential either individually or in combination with romidepsin, an extensively clinically tested LRA. We showed that ALKBH5 inhibitor 3 (ALKi-3) potentiated romidepsin-mediated viral reactivations both in vitro and ex vivo models of latency. Furthermore, we observed that ALKi-3 directly affects m^6A methylation on reactivated HIV-1 RNA. Our study provides a

proof-of-concept that the modulation of the m^{6}A pathway, specifically through the inhibition of ALKBH5, enhances HIV-1 reactivation from latency.

Methods

Cell lines

J-Lat A2 cells are derived from Jurkat T cells latently infected with the Tat-IRES-GFP vector, while J-Lat 10.6 and J-Lat 9.2 cells are derived from Jurkat T cells latently infected with the HIV-1 strain R7/E-/GFP [45]. U1 cells are latently infected with HIV-1 isolate NY5 and derived from promonocyte cell line U937 [46]. J-Lat A2, J-Lat 9.2, J-Lat 10.6 and U1 were sourced from the NIH Research and Reference Reagent Program and are cultured in Roswell Park Memorial Institute medium (RPMI 1640; Gibco #11875093) with 10% fetal bovine serum (FBS; Gibco #A5256801), and penicillin/streptomycin (PAN Biotech #P06-07100). Human embryonic kidney cells HEK 293T (ATCC #CRL-3216) were maintained in Dulbecco's Modified Eagle's medium (DMEM; Gibco #11965-092) supplemented with 5% FBS and penicillin/streptomycin.

Primary CD4$^+$ T cells model of HIV-1 infection

CD4$^+$ T cells were isolated from elutriated lymphocytes obtained from healthy donors using EasySep™ Human CD4$^+$ T cell isolation kit (StemCells Technologies, #17952) following the manufacturer's instructions. Isolated CD4$^+$ T cells were cultured in complete RPMI and stimulated with 5 µg/ml phytohemagglutinin-P (PHA-P; Sigma-Aldrich, #L1668) and 20 U/ml interleukin-2 (IL-2; Sigma-Aldrich, #H7041) for three days. Next, cells were spinoculated for two hours at 1200 × g at room temperature, washed and cultured in complete RPMI supplemented with IL-2. After 24 h, cells were treated with 50 µM of ALKi-3. Next day cells and extracellular culture supernatant were harvested for HIV-1 gene expression evaluation.

Cellular metabolic activity assay

Cellular metabolic activity was assessed utilizing a colorimetric XTT assay (Biological Industries, Cat. #20-300-1000) according to the manufacturer's instructions. Absorbance measurements were recorded with a microplate reader (SpectraMax iD5, Molecular Devices).

Flow cytometry

J-Lat A2, J-Lat 9.2, J-Lat 10.6 and primary CD4$^+$ T cells were harvested 24 h post-stimulation. The cells were washed with PBS and suspended in 3.7% paraformaldehyde (PFA; Sigma, Cat. #P6148) in PBS for fixation. Following a 30-minute fixation period, the cells were washed twice with PBS and resuspended in PBS. The percentage of GFP + cells was determined using a BD LSR Fortessa flow cytometer.

Virus production assays

HIV-1 production was measured in the supernatant of the J-Lat 9.2, J-Lat 10.6, U1 and primary CD4$^+$ T cell cultures by determining the CA-p24 levels by ELISA (Xpress Bio #XB-1000).

RNA extraction and quantification

Extracellular HIV-1 RNA was extracted from 200 µl of culture supernatant from J-Lat 9.2, J-Lat 10.6, U1 and primary CD4 + T cells at 24 h post-stimulation. The HIV-1 RNA isolation was performed automatically using the MagnifiQ 96 Pathogen instant kit (A&A Biotechnology, Poland) and the KingFisher Flex System (Thermo Fisher Scientific, Poland) according to the manufacturer's instructions. HIV-1 RNA was then reverse transcribed using the High Capacity cDNA Reverse Transcription Kit (Thermo Scientific, Cat. #4368814). The resulting cDNA was quantified by TaqMan-based qPCR using gag-p24 primers (gag-p24 forward: TCTCGACGCAGGACTC G, gag-p24 reverse: TACTGACGCTCTCGCACC) and probe (gag-p24 probe: 6-FAM-CTCTCTCCTTCTAG CCTC-MGB-NFQ), along with the RT PCR Mix Probe (A&A Biotechnology, Cat. #2008-2000P) and expressed as HIV-1 RNA copies/ml of the supernatant.

Cell-associated total RNA was extracted using TRIzol Reagent (Thermo Scientific, Cat. #15596018) according to the manufacturer's instructions and subsequently treated with TURBO DNase (Thermo Scientific, Cat. #AM2238). Next, 500 ng of total RNA was reverse transcribed using the High-Capacity cDNA Reverse Transcription Kit (Thermo Scientific, Cat. #4368814). The resulting cDNA was subjected to SYBR Green-based qPCR using GO-Taq MM (Promega, Cat. #A6002). qPCR was performed with primers targeting initiated transcripts (TAR: Forward, 5'-GTCTCTCTGG TTAGACCAG-3' and Reverse, 5'-TGGGTTCCCTA-GYTAGCC-3') and elongated transcripts (RRE: Forward, 5'-TGGGTTCCCTAGYTAGCC-3' and Reverse, 5'-TGGGTTCCCTAGYTAGCC-3'). The cDNA levels were quantified and normalized to GAPDH mRNA levels.

Study subjects

We selected six HIV-1-infected individuals at the St-Pierre Hospital (Brussels, Belgium) based on the following criteria: all volunteers were treated with ART for at least 1 year, had an undetectable plasma HIV-1 RNA level (20 copies/ml) for at least 1 year and had a level of CD4$^+$ T lymphocytes higher than 300 cells/mm3 of blood. Characteristics (age, CD4$^+$ T cell count, CD4$^+$ nadir, antiviral regimens, duration of therapy, duration

with undetectable plasma HIV-1 RNA level, and HIV-1 subtypes) of PLWH from the St- Pierre Hospital were well documented and are presented in the Supplementary Table 1.

Isolation of CD8$^+$-depleted PBMCs

CD8$^+$-depleted PBMCs used in reactivation assays were isolated from fresh whole blood of HIV$^+$ PLWH as previously described [16, 47]. For each treatment, six million CD8$^+$-depleted PBMCs were seeded in LymphoONE T-Cell Expansion Xeno-Free Medium (Takara). One day after isolation, cells were mock-treated or treated with a PMA/ionomycin cocktail (Invitrogen, #00-4970-03) as a positive control or by compounds for six days. Medium was harvested at day three and used for quantification of HIV-1 RNA. Cells were cultured in the presence of antiretrovirals [Efavirenz (100nM), Zidovudine (180nM), Raltegravir (200nM)].

Quantification of total HIV-1 DNA

The total cellular DNA was extracted from CD8$^+$-depleted PBMCs from PLWH using the QIA amp DNA Mini kit (Qiagen). The total cell-associated HIV-1 DNA was then quantified by ultra-sensitive real-time PCR (Generic HIV DNA cell kit, Biocentric) according to the manufacturer's instructions.

Quantitative assessment of HIV-1 RNA from culture supernatants of patient cells

Six days after drug treatment, culture supernatants from patient CD8$^+$-depleted PBMCs ex vivo cultures were collected for RNA extraction using QIA amp Viral RNA Mini kit (Qiagen). HIV-1 RNA levels were quantified using the Generic HIV Charge Virale kit (Biocentric) according to the manufacturer's instructions (detection limits of 75 HIV-1 RNA copies/ml).

Designing of lentiviral CRISPR guide, lentivirus production, and transduction in cells

Using CHOPCHOP platform we designed three CRISPR guide against ALKBH5 gene and synthesized by Genomed, Warsaw, Poland. Subsequently CRISPR guides were cloned in a lentiviral vector CRISPR v2 and recombinant clones were confirmed by sequencing with Genomed. Lentiviruses were produced in HEK293T cells by using a PEI co-transfection of CRISPR lentivirus plasmid CRISPR v2 along with packaging plasmid pSPAX2 and envelop plasmid pMD2G. Sixteen hours post-transfection DMEM medium was replaced with complete RPMI medium. The lentiviral particles were collected 48- and 72-hours post-transfection, filtered through 0.22 µm syringe filter (TPP #99722), and concentrated 40-times using Amicon® Ultra-15 Centrifugal Filter Unit 10 kDa MWCO (Merck Millipore #UFC901024), aliquoted and stored in -150 °C freezer.

The J-Lat 9.2 and U1 cells were transduced by CRISPR lentivirus targeting ALKBH5 genes by performing spinoculation (800 × g, 90 min, 32 °C), using 10 µg of lentiviral particles (MOI 10) per 1×10^6 cells, in presence of polybrene (8 µg/ml), in total 100 µl of RPMI. After spinoculation, lentivirus containing medium was removed and cells were maintained at a concentration of 1×10^6 cells/ml in complete RPMI medium. Sixteen hours post-transduction cells were diluted and maintained in complete RPMI medium containing 1 µg/ml of puromycin (BioShop #PUR555.2) for five days. After antibiotic selection, ALKBH5 depleted cells were ready to use for further experiments.

Western blot

Cells were lysed in RIPA lysis buffer (50 mM TRIS-HCL pH 7.4, 150 mM NaCl, 1% NP-40, 0.1% SDS, 1.5 mM MgCl2, 1 mM PMSF, 0.1 mg/ml Dextran, Protease inhibitor cocktail) for 30 min at 4 °C followed by collection of the lysates. Equal amounts of lysates were used for SDS PAGE. Western blot was performed with primary antibodies: rabbit anti-ALKBH5 (1:1000; Sigma #HPA007196), rabbit anti-GAPDH (1:1000; Cell Signaling Technology #2118), and secondary goat anti-rabbit (1:20000; Sigma # A0545). The signal was developed by Azure biosystems 600 using ECL reagent (Thermo Scientific #32106).

Immuno-RNA-FISH and confocal imaging

U1 cells were collected 24 h post-stimulation, centrifuged, and immobilized on poly L-lysine-coated coverslips by incubating for one hour in RPMI with 50% FBS. Cells were washed with DPBS, fixed in 3.7% PFA for 30 min, and permeabilized in PBST (0.1% Tween 20 in PBS) for 10 min. RNA FISH was performed using Molecular Instruments' HCR™ RNA-FISH protocol with probes targeting the HIV-1 gag p24 region. Cells were pre-incubated with 30% Probe Hybridization Buffer for 30 min at 37 °C, followed by incubation with p24 probes in the same buffer at 37 °C for 16 h. Post-hybridization, cells were washed in warm 30% Wash Buffer four times and in 5x SSCT buffer twice. Amplification was initiated by pre-incubating cells in Amplification Buffer for 30 min at room temperature. Amplifiers B1-h1 and B1-h2, conjugated with Alexa Fluor 647, were prepared by snap-cooling post heat shock at 95 °C for 90 s. Amplification occurred at room temperature with a 1:50 dilution of amplifiers in amplification buffer for 16 h. Post-amplification, cells were washed five times in 5x SSCT and twice in PBS. Next, cells were blocked in 5% BSA in 0.1% PBST and incubated overnight at 4 °C with m^{6}A antibody (Abcam, 1:200) in 1% BSA in 0.1% PBST. After washing

with 0.1% PBST three times, cells were incubated with secondary anti-rabbit Alexa Fluor 594 antibody (Thermo Scientific, 1:400) in 1% BSA in 0.1% PBST for one hour at 37 °C. Nuclei were stained with DAPI and slides were mounted using Prolong Diamond Antifade Mounting Medium. Images and Z-stacks were acquired by confocal microscope ZEISS LSM 880 with 100x/1.46 NA Plan Apochromat Objective with oil immersion and the ZEN Imaging Software (ZEISS), and analyzed using Fiji software. To quantify the number and volume of spots, after being imported via the Bio-Formats plugin [48], the images were segmented, and 3D structures larger than 5 voxels were subsequently identified using the 3D Object Counter plugin [49].

m^{6}A-Modified RNA Immunoprecipitation

U1 cells were treated with either romidepsin (5 nM) or romidepsin (5 nM) in combination with ALKi-3 (100 µM) for 24 hours. Total RNA was extracted using TRIzol Reagent according to the manufacturer's instructions and subsequently treated with TURBO DNase. From the total RNA, mRNA was enriched using GenEluteTM mRNA Miniprep Kit (Merck #MRN70). Obtained mRNA was concentrated using RNeasy MinElute Cleanup Kit (Qiagen #74204) prior to RNA fragmentation. For meRIP (Magna MeRIP m^{6}A Kit, #17-10499, Millipore) fragmented mRNA was incubated for 2 hours at 4°C, with either anti-N6-methyloadenosine (m^{6}A) antibody (clone 17-3-4-1, #MABE1006, Merck) or normal mouse IgG antibody (#CS200621, Merck, negative control) previously coupled with A/G-coated magnetic beads. Samples were placed on a magnetic stand and the unbound RNA was discarded. The beads were then washed three times with IP buffer and bound RNA was released by two rounds of 1 hour elution in IP buffer supplemented with 20 mM m^{6}A sodium salt. RNA was purified and concentrated in 20 µl of water, using RNeasy MinElute Cleanup Kit. RT-qPCR was performed on the purified RNA targeting known m^{6}A methylated region of EEF1A1 cellular gene mRNA (positive control: FP 5'–CGGTCTCAGAACTGTTTGTTTC–3', RP 5'–AAACCAAAGTGGTCCACAAA–3'), and its region unaffected by m^{6}A methylation (negative control: FP 5'–GGATGGAAAGTCACCCGTAAG–3', RP 5'–TTGTCAGTTGGACGAGTTGG–3').

Statistical analysis

In in vitro studies, at least three independent experiments in duplicate repeats were performed for each condition examined. Mean values are shown with the standard error of the mean (SEM) and statistical significance was measured with a Student's *t* test. Significant *p* values are indicated by the asterisks above the graphs ($p \le 0.05$ [*], $p \le 0.01$ [**], ≤ 0.001 [***], ≤ 0.0001 [****]). Analyses were performed using Prism version 9.0.

Results

Screening of compounds modulating the activities of METTL3-METTL14-WTAP complex, ALKBH5 and FTO in reactivation of HIV-1 from latency

To assess the role of the m^{6}A pathway in HIV-1 reactivation, we took advantage of previously published inhibitors of ALKBH5 [50], FTO [50] and activators of METTL3-METTL14-WTAP complex [44]. These compounds (Fig. 1A) were developed by M. Karelson's group using virtual screening assays coupled with molecular docking against either FTO (inhibitor 1 and inhibitor 2 from [50]), ALKBH5 (inhibitor 3 and inhibitor 4 from [37]), or METTL3-METLL14 complex (activators 1–4 from [44]). Firstly, we tested the cytotoxicity of these 8 compounds ranging from 1 to 500 µM in CD4$^+$ T lymphoid cell lines i.e., SupT1 and in in vitro cellular model of latency, the J-Lat A2 (Suppl. Figure 1A-B, respectively) that harbors a mini-reporter provirus containing the *gfp* reporter gene [45]. We assessed that the maximal non-toxic dose of compounds was 100 µM (Supple. Figure 1A-B). Next, we evaluated the potential reactivation potential of the compounds used alone or in combination with well-characterized LRA, romidepsin for which we determined the sub-optimal dose in J-Lat A2 latency model (Suppl. Figure 2A.). Next, we performed an initial screening of the compounds used alone or in combination with romidepsin in J-Lat A2. The percentages of GFP$^+$ cells in J-Lat A2 were measured by flow cytometry (Fig. 1B-C). Single compound treatments did not induce the viral reactivation, whereas the combined treatment of ALKBH5 inhibitor, inhibitor 3 (named here ALKi-3) with romidepsin increased viral reactivation when compared to romidepsin alone (Fig. 1C). Moreover, ALKi-3 combined treatment with romidepsin increased the median fluorescent intensity (MFI) of GFP$^+$ cells (Suppl. Figure 2B). We though selected ALKi-3 for further studies.

ALKBH5 inhibitor, ALKi-3 enhances reactivation potential of Romidepsin in in vitro cellular latency models of lymphocytic and monocytic origins

Next, we wished to further characterize the reactivation potential of combinatory treatment of ALKi-3 with romidepsin in two well-studied HIV-1 latency cellular models of T-lymphoid (J-Lat 9.2) and promonocytic (U1) origins. J-Lat 9.2 cell line harbors near-full-length HIV-1 provirus containing the *gfp* reporter gene in place of *nef* and frameshift mutation in *env*. U1 cells are chronically HIV-1 infected monocytic (U937) cells that contain full-length HIV-1 genome. Firstly, a range of romidepsin doses was selected (based on the previously published study of Bouchat et al. [18]) to determine its suboptimal dose for combinatory treatments with ALKi-3 in both models, in order to assess the potential beneficial effect of this combination. As shown in Suppl.

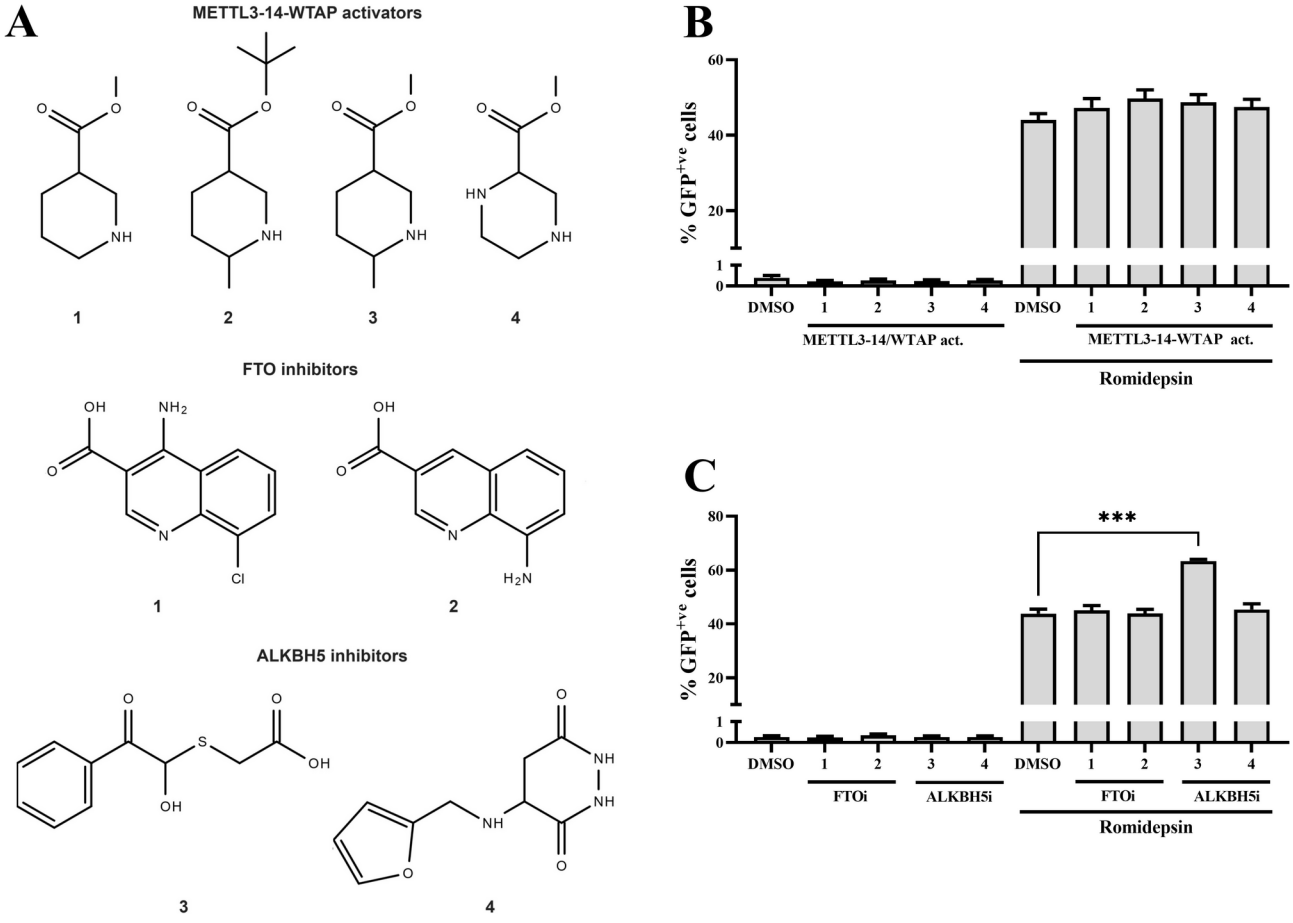

Fig. 1 ALKBH5 inhibitor 3 (ALKi-3) potentiates viral reactivation mediated by a sub-optimal dose of romidepsin. (**A**). Chemical structures of the METTL3-14-WTAP activators, FTO inhibitors, and ALKBH5 inhibitors. **(B-C)** J-Lat A2 cells were either DMSO-treated, treated with 100 µM of indicated compounds alone or in combination with romidepsin [5 nM]. At 24 h post-treatment, viral reactivation was assessed by flow cytometry to quantify the percentages of GFP$^+$ cells. Means and standard error of means from three biological replicates in duplicates are indicated. Statistical analysis was performed using a paired Student's *t*-test, $p \leq 0.0002$ (***)

Figure 3A and 3B, increasing doses of romidepsin correlated in a dose-dependent manner with the percentages of GFP$^+$ cells (in case of J-Lat 9.2) and with the levels of extracellular HIV-1 RNA (in case of U1) at 24 h post-treatment. Based on the reactivation data, we selected 17.5 nM in J-Lat 9.2 and 5 nM in U1 as suboptimal doses of romidepsin (Suppl. Figure 3A and 3B, respectively). Next, we evaluated the reactivation potential of increasing doses of ALKi-3 with sub-optimal dose of romidepsin. As shown in Fig. 2A and F, ALKi-3 potentiated the reactivation capacity of romidepsin in a dose-dependent manner in J-Lat 9.2 and U1, respectively, with marginal effect on cellular metabolic activity except for 200 µM dose in J-Lat 9.2 cells (Fig. 2B and G). Next, we further evaluated the effect of ALKi-3 in J-lat 9.2 and we showed that combined treatment nearly doubled the percentages of GFP$^+$ cells (Fig. 2C), increased the MFI of GFP$^+$ cells (Suppl. Figure 3C), levels of extracellular p24 capsid as measured by ELISA (Fig. 2D) as compared with the individual romidepsin treatment. We also measured the levels of intracellular TAR- and RRE-containing HIV-1 transcripts that also increased by 2-fold in romidepsin + ALKi-3 combined treatments compared with romidepsin alone (Fig. 2E). To further strengthen these observations, we used another J-Lat clone, J-Lat 10.6, in which we tested ALKi-3 in combination with increasing doses of romidepsin, as determined in Suppl. Figure 4A. As shown in Suppl. Figures 4B and 4C, ALKi-3 combined with lower doses of romidepsin (2.5 and 5 nM) exhibited greater potency in viral reactivation compared to romidepsin alone. This was assessed by flow cytometry measuring the percentages of GFP$^+$ cells (Suppl. Figure 4B), levels of extracellular p24 capsid protein as measured by ELISA (Suppl. Figure 4C), and genomic HIV-1 RNA levels in the culture supernatant (Suppl. Figure 4D). However, no potentiated effect of ALKi-3 was observed when higher dose of romidepsin (10 nM) was used, supporting the notion of dose saturation (Suppl. Figure 4B-D).

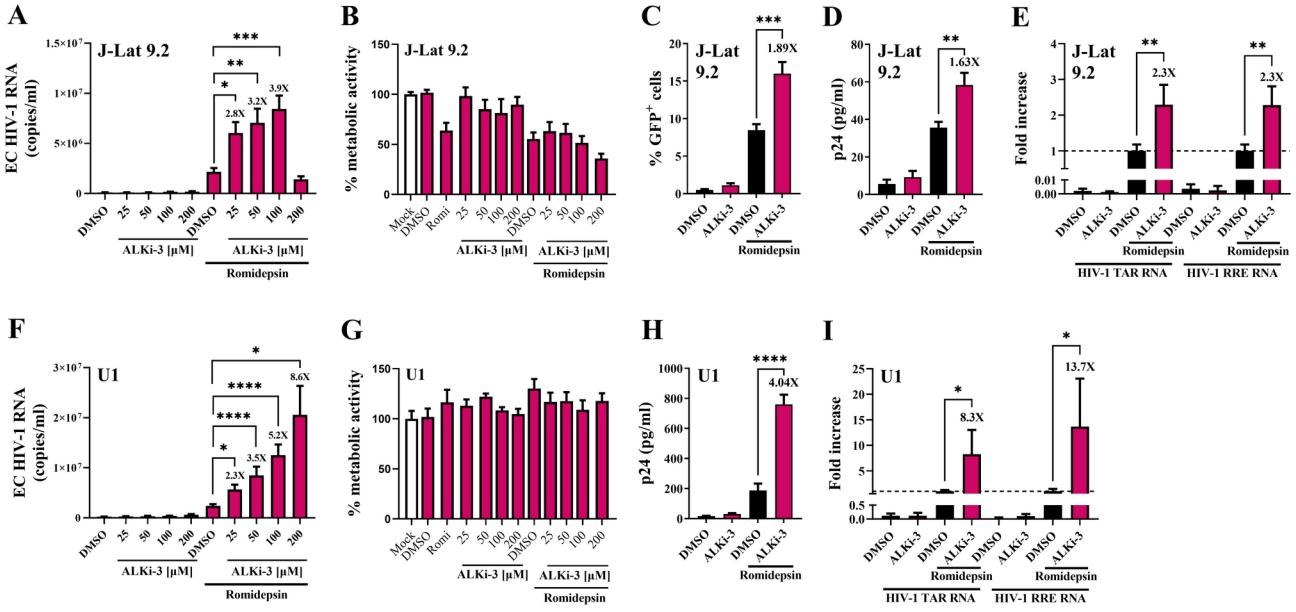

Fig. 2 Enhanced reactivation potential of romidepsin by ALKi-3 in lymphoid J-Lat 9.2 and promonocytic U1 in vitro latency cellular models. (**A-B**, **F-G**) J-Lat 9.2 and U1 cells were either DMSO-treated, treated with increasing doses of ALKi-3 [25-50-100-200 μM] alone or in combination with sub-optimal dose of romidepsin (17.5 nM, and 5 nM for J-Lat 9.2 and U1 cells, respectively). At 24 h post-treatment **(A**, **F)** viral reactivation was assessed by measuring the concentration of genomic viral RNA copies/ml in culture supernatant using RT-qPCR. **(B**, **G)** Cells metabolic activity was measured by using XTT assay. Results obtained with the mock-treated cells were arbitrary set at a value of 100%. **(C-E**, **H-I)** Cells were treated with either DMSO (control), ALKi-3 alone (100 μM), or in a combination with suboptimal dose of romidepsin (17.5 nM, and 5 nM for J-Lat 9.2 and U1 cells, respectively). Viral reactivation was assessed 24 h post-treatment. **(C)** J-Lat 9.2 cells were subjected to flow cytometry analysis to quantify the percentages of GFP^+ cells. **(D**, **H)** Viral production was estimated by measuring CA-p24 antigen in culture supernatant. **(E**, **I)** Total RNA was extracted that was subsequently subjected to quantification by RT-qPCR for TAR- and RRE-containing HIV-1 RNAs. Values were normalized using *gapdh* primers and were presented as relative fold changes to the values measured in romidepsin + DMSO-treated cells which were arbitrarily set at a value of 1. **(A-I)** Means and standard errors of the means from three biological repetitions in duplicates are represented. Statistical analysis was performed using a paired Student's *t*-test with *p*-values indicating the significance level: $p \leq 0.05$ (*), $p \leq 0.002$ (**), $p \leq 0.0002$ (***), and $p \leq 0.0001$ (****)

Next, we addressed the reactivation potency of ALKi-3 with romidepsin in U1 monocytic cells. We showed that ALKi-3 increased the potency of romidepsin by 4-fold when extracellular p24 capsid levels were measured by ELISA (Fig. 2H). Interestingly, ALKi-3 strongly upregulated the romidepsin-induced intracellular levels of TAR- and RRE-containing HIV-1 RNA by 8.3-fold and 13.7-fold, respectively, compared with romidepsin alone (Fig. 2I). Moreover, we showed that potencies of suboptimal doses of another LRA, TNFα could also be augmented by ALKi-3 co-treatment in J-Lat A2, J-Lat 9.2 and U1 cells (Suppl. Figure 5).

Our results collectively demonstrated that combining romidepsin with the ALKBH5 inhibitor ALKi-3 potentiated viral reactivation across all - cell lines tested, with latent proviruses in U1 cells being more prone to reactivation by ALKi-3 and romidepsin than those in J-Lat clones.

Depletion of ALKBH5 mimicked the effects of ALKi-3 in potentiating viral reactivation in in vitro latency models

To confirm that modulation of ALKBH5 potentiates viral reactivation with romidepsin, we depleted ALKBH5 by CRISPR/Cas9 approach in J-Lat 9.2 and U1 cells. The potency of ALKBH5 knockout was validated by Western blot in J-Lat 9.2 and U1 cells as shown in Fig. 3A and E, respectively. Next, we assessed viral reactivation in both cell lines upon ALKBH5 depletion. As shown in Fig. 3B, ALKBH5 depletion in J-Lat 9.2 cells increased romidepsin potency by 1.7-fold as assessed by flow cytometry and increased the MFI of GFP^+ cells (Suppl. Figure 6). Levels of extracellular p24 capsid levels increased by 1.8-fold as measured by ELISA compared with romidepsin alone (Fig. 3C). Of note, intracellular viral RNA remained unchanged compared with romidepsin alone (Fig. 3D). In addition, depletion of ALKBH5 in U1 cells potentiated romidepsin activity in viral reactivation by 1.6-fold in p24 capsid levels measured by ELISA (Fig. 3F). Moreover, levels of TAR and RRE-containing HIV-1 transcripts increased by 1.5-fold and 2.6-fold, respectively.

ALKi-3 treatment potentiates HIV-1 gene expression in primary $CD4^+$ T cell model of HIV-1 infection

Building on our observation that ALKBH5 inhibition potentiated LRA-mediated latency reactivation, we sought to investigate the effect of ALKi-3 on HIV-1 gene

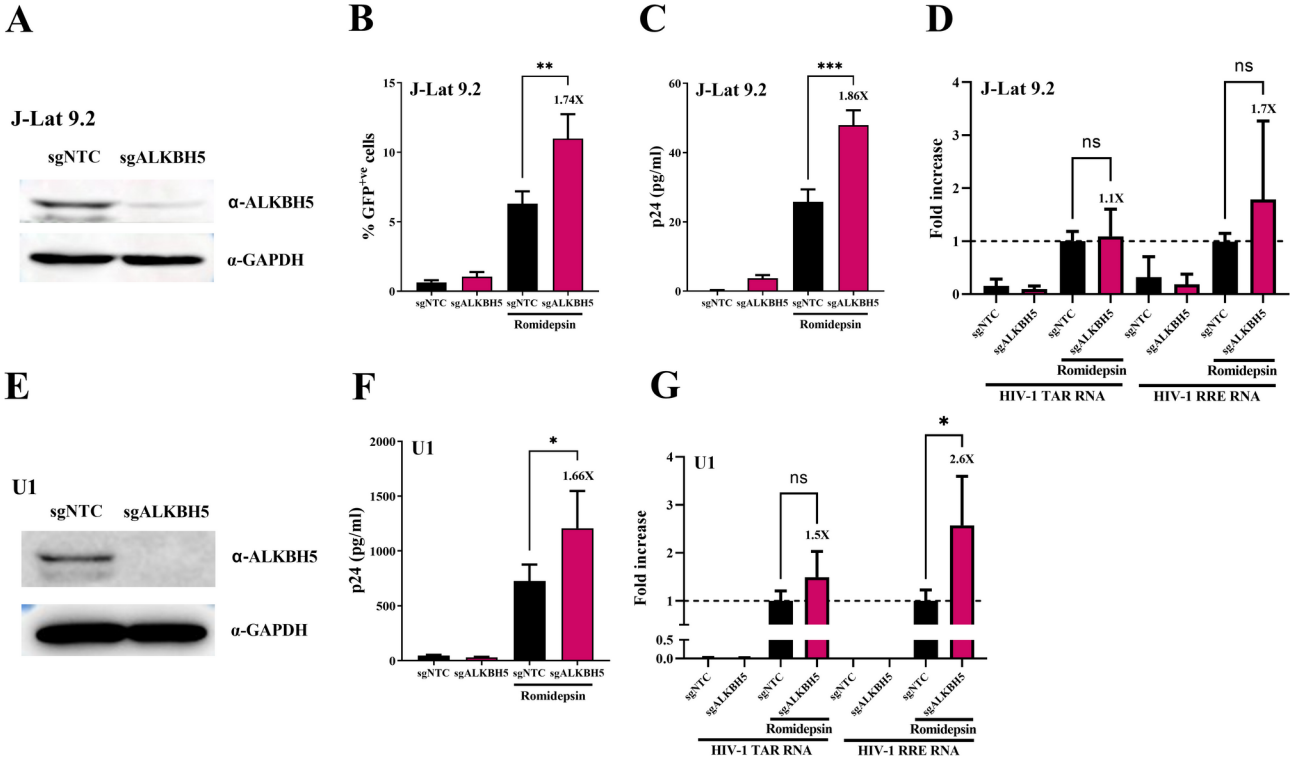

Fig. 3 Depletion of ALKBH5 potentiates viral reactivation in in vitro latency models. The J-Lat 9.2 **(A-D)** or U1 **(E-G)** cells were transduced with lentiviral vector targeting ALKBH5 (sgALKBH5) or with control sgRNA (sgNTC). Five days after puromycin selection, ALKBH5-depleted cells were harvested and subjected to romidepsin treatment for additional 24 h. **(A**, **E)** Immunoblotting to detect ALKBH5. GAPDH is the protein loading control. **(B)** J-Lat 9.2 cells were subjected to flow cytometry analysis to quantify the percentage of GFP$^+$ cells. **(C**, **F)** Viral production was estimated by measuring CA-p24 antigen in culture supernatant. **(D**, **G)** Total RNA was extracted and subsequently subjected to quantification by RT-qPCR for TAR- and RRE-containing HIV-1 RNA. Values were normalized using *gapdh* primers and were presented as relative fold changes to the values measured in romidepsin treated sgNTC-transduced cells which were arbitrarily set at a value of 1. **(B**, **C**, **F)** Means and standard errors of the means from three biological repetitions in duplicates are represented. Statistical analysis was performed using a paired Student's *t*-test with *p*-values indicating the significance level: $p \leq 0.05$ (*), $p \leq 0.002$ (**), $p \leq 0.0002$ (***)

expression in more physiological model of primary CD4$^+$ T cells infected with HIV-1. To this end, CD4$^+$ T cells were isolated from elutriated lymphocytes obtained from three healthy donors. Purity of the CD4$^+$ T cells was confirmed by CD3 and CD4 staining (Suppl. Figure 7). Next, CD4$^+$ T cells were cultured in the presence of PHA-P and IL-2 for three days, then infected with VSV-G pseudotyped HIV-1 molecular clone (NL4-3 ΔEnv_EGFP). Next, cells were treated or not with ALKi-3 for additional 24 h and then subjected to assess the effect on the virus reactivation (Fig. 4A). As shown in Fig. 4, ALKi-3 treatment increased the percentages GFP$^+$ cells (Fig. 4B-C) and the MFI of GFP$^+$ cells (Fig. 4D). Additionally, ALKi-3 treatment led to an increase in viral production as measured by p24 ELISA (Fig. 4E) and upregulated intracellular TAR HIV-1 RNA transcripts as assessed by RT-qPCR (Fig. 4F). These findings highlight that ALKi-3 enhances HIV-1 gene expression and production in primary CD4$^+$ T cell model of HIV-1 infection.

Evaluation of the combined treatment of Romidepsin with ALKi-3 in CD8$^+$-depleted PBMCs from ART-treated aviremic PLWH

Next, we assessed whether combined treatment of romidepsin with ALKi-3 also correlated with HIV-1 recovery in ex vivo cultures of CD8$^+$-depleted PBMCs isolated from ART-treated aviremic PLWH. Firstly, we tested the cytotoxicity of increasing doses of ALKi-3 in PBMCs from healthy donors and showed that 100μM dose is not toxic (Suppl. Figure 8). Next, we isolated CD8$^+$-depleted PBMCs from six ART-treated aviremic PLWH; purified cells were subsequently mock-treated, treated with PMA/Ionomycin cocktail as a positive control for global T cell activation or with ALKi-3, romidepsin, or a combination of romidepsin with ALKi-3. Cell-associated total HIV-1 DNA and extracellular viral RNA were quantified in culture supernatants. As shown in Table 1, ALKi-3 alone did not increase the recovered viral genomic RNA, while romidepsin caused increases in 4 out of 6 patients cell cultures and PMA/Ionomycin treatment caused increases in 5 out of 6. In the case of combinatory romidepsin + ALKi-3 treatment we

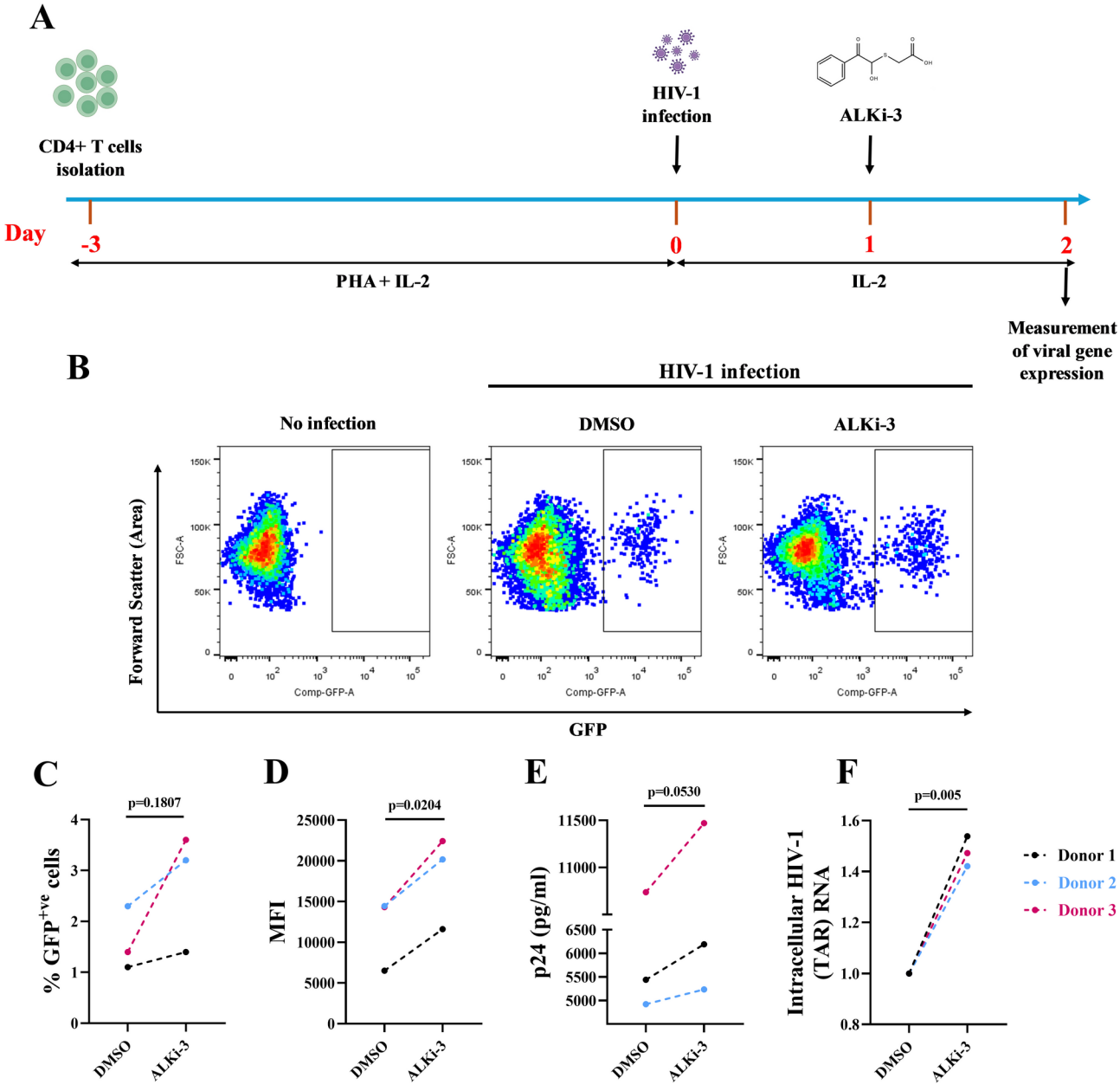

Fig. 4 ALKi-3 treatment potentiates HIV-1 gene expression in primary CD4$^+$ T model of HIV-1 infection. **(A)** Schematic of the experiment. CD4$^+$ T cells were isolated and stimulated with 5 µg/ml of PHA-P and 20 units/ml of IL-2 for three days. At day three, CD4$^+$ T cells were infected with HIV-1 NL4-3 ΔEnv_EGFP and after 24 h of HIV-1 infection cells were treated with 50 µM of ALKi-3 for further 24 h and subjected to HIV-1 expression analyses. **(B)** Representative flow cytometry dot plot depicting no infection, and cells infected with HIV-1 NL4-3 ΔEnv_EGFP either treated with DMSO or ALKi-3. CD4$^+$ T cells were subjected to flow cytometry analysis to quantify the percentage of GFP$^+$ cells (**C**) and their MFI (**D**). **(E)** Viral production was estimated by measuring CA-p24 antigen in culture supernatant. **(C– E)** Means and standard errors of the means from three donors are represented. Statistical analysis was performed using two-way *ANOVA* with *p* value indicated above the graph **(F)** Total RNA was extracted and subsequently subjected to quantification by RT-qPCR for TAR-containing HIV-1 RNA. Values were normalized using *gapdh* primers and were presented as relative fold changes to the values measured in DMSO-treated cells which were arbitrarily set at a value of 1. Means and standard errors of the means from three donors are represented. Statistical analysis was performed using a paired Student's *t*-test with *p* value indicated above the graph

observed potentiated viral recovery in 2 out of 6 patients, when compared to individual treatments, underscoring that in some patients cells we could appreciate the potentiated effect of ALKi-3 over romidepsin.

ALKBH5 inhibition increases the levels of m^{6}A methylated HIV-1 RNA

Next, we attempted to assess the impact of ALKi-3 on m^{6}A methylation in HIV-1 RNA. To this end, we performed an meRIP on mRNA from U1 cells treated with

Table 1 Evaluation of viral recovery in ex vivo cultures of $CD8^+$ depleted PBMCs from six ART-treated HIV^+ aviremic PLWH. Ex vivo cultures of $CD8^+$-depleted PBMCs from six ART-treated HIV^+ PLWH were mock treated, treated with ALKi-3 [100µM], Romidepsin [17.5nM], combined ALKi-3 + Romidepsin or with a with PMA/I cocktail as a positive control (C+) in the presence of ARV [280 nM Ritonavir, 180 nM Azidothymidine, 200 nM Raltegravir, 100 nM efavirenz]. Three days post-treatment, concentrations of genomic viral RNA in culture supernatants were determined and the values were expressed as HIV-1 RNA copies/ml. Total HIV-1 DNA was expressed as HIV-1 DNA copies/10^6 $CD8^+$-depleted PBMCs. Values representing higher viral production after the combined treatment than after the single drug treatments are shown in grey. '/' indicates below the 75 HIV-1 RNA copies/ml limit of detection

Patient	total HIV-1 DNA (copies/10^6 PBMCs)	mock	Romi	ALKi-3	Romi+ALKi-3	C+
P1	120	/	279	/	/	251
P2	242	/	151	/	946	542
P3	125	756	395	128	1396	441
P4	145	1249	1118	426	694	5154
P5	14	/	709	/	/	713
P6	762	707	6382	927	3621	2389

a suboptimal dose of romidepsin alone or in combination with ALKi-3 using either an m^6A-specific antibody or a non-specific IgG antibody as a control. The immunoprecipitated RNA was then analyzed using RT-qPCR against the cellular gene EEF1A1 (as a positive control) and the RRE-containing HIV-1 RNA. To determine the m^6A fold enrichment on RNA, we normalized the values to the input samples and antibody control samples. Our results showed an m^6A enrichment on cellular RNA and viral RNA in combined treatment compared with romidepsin alone (Fig. 5A and B, respectively), indicating that ALKi-3 augments the levels of m^6A -methylated HIV-1 RNA. Next, to corroborate the meRIP data, we established an immuno-RNA FISH protocol for m^6A and HIV-1 RNA in U1 cells. We detected numerous spots of HIV-1 RNA that colocalized with m^6A staining (Fig. 5C). Next, to assess the effect of ALKi-3 on HIV-1 RNA, we reactivated U1 cells with romidepsin or with combined treatment of romidepsin with ALKi-3 followed by immuno-RNA FISH. Confocal images were analyzed to quantify the number of m^6A and HIV-1 RNA spots. As shown in Fig. 5D and E, we observed statistically significant increases in the numbers of m^6A and viral RNA spots, respectively. Importantly, we observed an increased colocalization between m^6A and HIV-1 RNA in combined ALKi-3 + romidepsin treatment compared with individual romidepsin (Fig. 5F), confirming meRIP results.

Discussion

The persistence of latent viral reservoirs remains one of the most formidable barriers to achieving an HIV-1 cure. HIV-1 latency is a complex phenomenon that is maintained by a series of intricate molecular mechanisms, including epigenetic, transcriptional, and less-characterized post-transcriptional blocks [7]. Indeed, several additional blocks to transcriptional elongation, polyadenylation, splicing [51, 52] and nucleocytoplasmic HIV-1 RNAs export [20, 53] in PLWH cells have been revealed, challenging the dogma that HIV-1 latency is mainly regulated at the transcriptional level. Notably, current LRAs employed in the "shock-and-kill" strategy primarily focus on relieving epigenetic and transcriptional blocks to reactivate latent viruses [8, 14, 16, 18]. However, the clinical efficacy of LRAs is limited, partly due to their inability to fully reverse latency and the lack of LRAs specifically targeting post-transcriptional mechanisms. Romidepsin, a pan-HDAC inhibitor, is an FDA-approved epigenetic drug used for treating cutaneous and peripheral T-cell lymphoma [54] and is also a potent LRA according to ex vivo studies [55]. Significant in vivo latency reversal was also observed for romidepsin alone [56] and in combination with 3BNC117 or Vacc-4x [57, 58]. We therefore choose romidepsin as proof-of-principle in combinatory studies with diverse small chemical compounds targeting the m^6A pathway. In recent years several groups have reported that depletion of the m^6A writer proteins METTL3 and METTL14 suppresses viral gene expression, while depletion of demethylase ALKBH5 enhances HIV-1 gene expression [28–31, 33]. Although the role of the m^6A pathway in HIV-1 latency and reactivation remains largely unexplored, a recent study by Mishra et al. provided evidence of its relevance by demonstrating a positive correlation between cellular RNA m^6A levels and HIV-1 latency reversal [59].

Here, we identified that an inhibitor of ALKBH5, ALKi-3, potentiated romidepsin-mediated latent viral reactivation in in vitro lymphoid and promonocytic models of HIV-1 latency and ALKi-3 treatment increased HIV-1 expression in primary $CD4^+$ T cell model of infection with HIV-1 molecular clone. This observation could build on "shock-and-kill" by addition of ALKi-3 inhibitor to enhance the "shock" at post-transcriptional level. Combining ALKi-3 can allow romidepsin to be administered at lower concentrations compared to romidepsin monotherapy. Potentially, this offers several advantages,

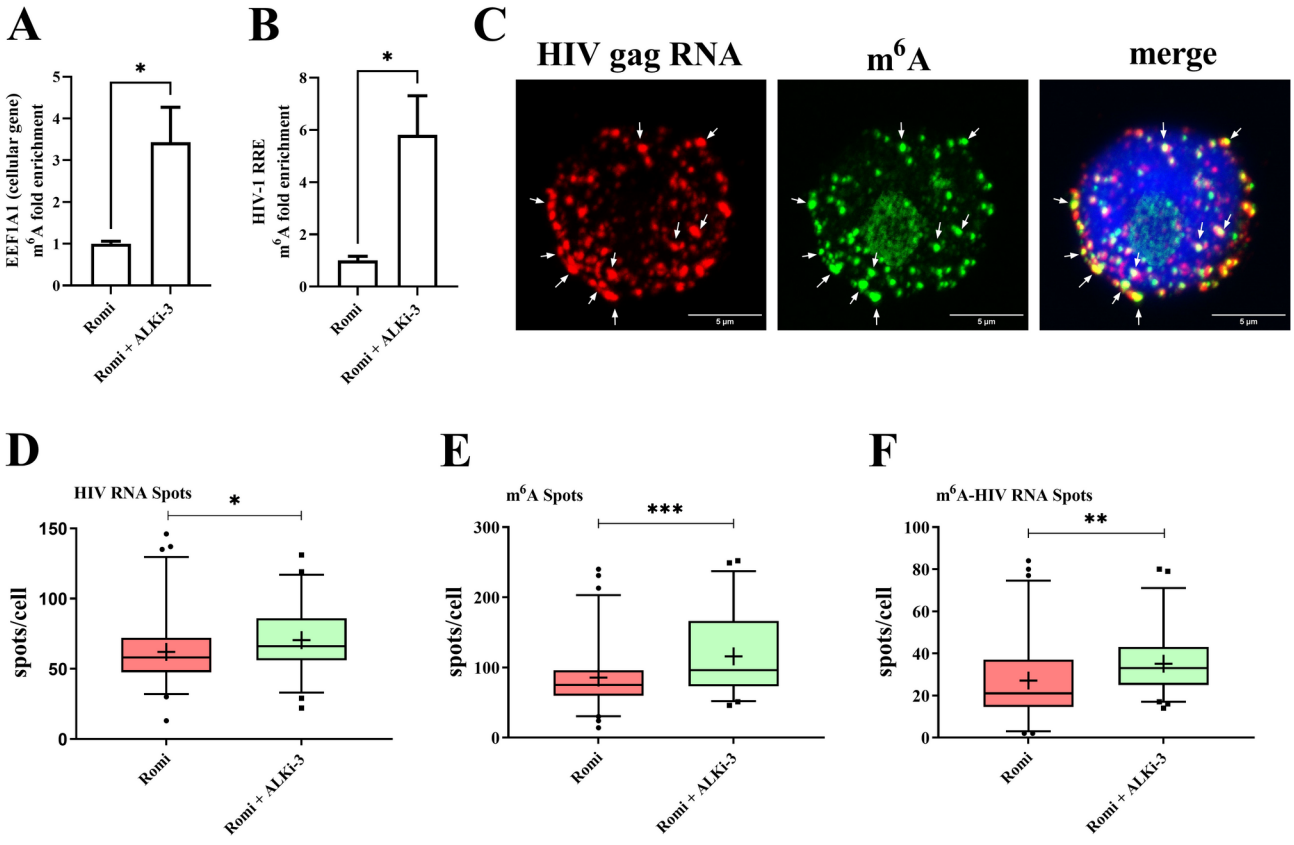

Fig. 5 Impact of ALKi-3 on the levels of m^6 A methylated HIV-1 RNA. U1 cells were treated either with romidepsin alone or with romidepsin + ALKi-3 and were collected 24 h post-treatment. **(A-B)** Total RNA was extracted and subsequently subjected to polyA mRNA enrichment followed by meRIP against m^{6}A modified RNA. The m^{6}A immunoprecipitated RNA was quantified by RT-qPCR for cellular EEF1A1- and RRE-containing HIV-1 RNAs. Values were normalized using input and IgG control and were presented as m^{6}A fold enrichment. Means and standard errors of the means from three biological repetitions are represented. Statistical analysis was performed using a paired Student's *t*-test with *p*-values indicating the significance level: $p \leq 0.05$ (*), $p \leq 0.002$ (**), $p \leq 0.0002$ (***), and $p \leq 0.0001$ (****). **(C-F)** Reactivated U1 cells were subjected to RNA-FISH and immunostaining using antibodies against m^{6}A modification for subsequent confocal microscopy analysis. **(C)** Representative image of m^{6}A immuno-HIV RNA FISH. HIV-1 ^{gag}RNA is shown in red, m^{6}A in green, and DAPI-stained nucleus in blue. Yellow spots indicate colocalization sites as marked by white arrows. **(D-F)** The number of m^{6}A **(D)**, HIV-1 ^{gag}RNA **(E)** and m^{6}A-HIV-1 ^{gag}RNA **(F)** spots were quantified. Images were acquired with confocal microscopy and spots were quantified in *z*-stacks from approx. 20 images/biological repetition, $n = 3$. Results are presented as box and whiskers with 5–95% confidence interval. Median value is shown as a bar, dots are spots outside the whiskers representing outliers, mean value is shown as "+".Statistical analysis was performed using a paired Student's *t*-test with *p*-values indicating the significance level: $p \geq 0.12$ (not significant– ns), $p \leq 0.05$ (*), $p \leq 0.002$ (**), $p \leq 0.0002$ (***), and $p \leq 0.0001$ (****)

such as minimizing toxicity and off-target effects [60, 61] while still achieving effective latency reversal - critical considerations for the clinical applicability of the "shock-and-kill" strategy. Moreover, even robust reactivation leaves the majority of the latent reservoir untouched posing a major obstacle to achieving functional cure (ref: https://doi.org/10.1016/j.cell.2013.09.020). Our study does not yet address this critical issue; rather, it offers a proof-of-concept for a potentially more tolerable regimen that may be optimized further.

Importantly, potentiated effect of combined ALKi-3 + romidepsin treatment was reproducible in ex vivo cultures of CD8$^+$-depleted PBMCs from 2 out of 6 ART treated HIV$^+$ aviremic PLWH. However, as in agreement with previous studies [18, 62], we observed the inter-patient variability in the reactivation capacity of proviruses in ex vivo cell cultures, highlighting the patient-specific nature of HIV-1 latent reservoir [7]. Interestingly, a recent elegant study by Tegowski et al., using a deamination adjacent to RNA modification targets (DART-seq) method to acquire a transcriptome-wide m^{6}A mapping at a single-cell level, unraveled an extreme heterogeneity in the frequency of individual m^{6}A sites across single cells [63]. Although many mRNAs contained a high number of total m^{6}A sites, most of these sites occurred in a small population of cells [63]. Thus, it is likely that only a small population of cells is frequently m^{6}A methylated which should be addressed by future single-cell approaches to address the correlation between HIV-1-latently infected cells and their reactivation capacities in the context of their m^{6}A methylation status. Interestingly, we observed that either pharmacological

inhibition or depletion of ALKBH5 had more robust impact on latent viral reactivation in promonocytic U1 than lymphocytic J-Lat cells, highlighting the heterogenous nature of latent reservoirs and the complexity of molecular mechanisms governing latency that might differ between different cell types.

The exact mechanism of ALKBH5-mediated negative regulation during latent viral reactivation remains elusive. It is well established that HIV-1 RNA has a higher number of m^{6}A modification sites compared to cellular RNAs [29, 64]. The very first work by Lichinchi et al. identified by meRIP-seq distinct m^{6}A-peaks located across the HIV-1 genome [28]. Notably, they found a peak in the Rev response element (RRE) and further showed that m^{6}A methylation enhanced Rev binding to RRE leading to increased viral RNA export, and subsequent increase in viral replication [28]. In our study, by using me-RIP coupled with RT-qPCR against RRE, we also observed increased m^{6}A-methylated RRE-containing HIV-1 RNA levels in combined romidepsin + ALKi-3 treatments compared to romidepsin alone. However, more studies are needed to dissect the potential effects of ALKi-3 on Rev-dependent export. Moreover, by using either meRIP-seq or photo-crosslinking-assisted m^{6}A sequencing (PA-m^{6}A-seq) approaches several other recent studies have identified multiple m^{6}A modifications present in *env/rev*, *nef*, *3' UTR*, *5' UTR*, *gag*, *pol*, *pol/nef*, and the packaging signal (ψ) regions [29, 30, 34, 65, 66]. However, techniques, such as meRIP-seq and PA-m^{6}A-seq reveal peaks of the m^{6}A modifications identified in fragmented RNA, thus do no provide a single-nucleotide resolution. Notably, a recent study by Baek et al. advanced the field by analyzing m^{6}A modifications on individual full-length HIV-1 RNAs with single nucleotide resolution using a Nanopore direct RNA sequencing (DRS) method [67]. This elegant study found that HIV-1 predominantly preserves functionally redundant m^{6}A sites at three DRACH motifs—A8079, A8975, and A8989—located near the 3' end of HIV-1 RNA. Mutations in all three m^{6}A sites led to increased splicing of unspliced (US) RNA, and significantly decreased their levels, reduced virion release, and lowered viral infectivity [67]. Moreover, Tsai et al. demonstrated that YTHDF2-recognition of m^{6}A modified HIV-1 transcripts can enhance their stability [31] contrary to YTHDF2 role in destabilizing cellular mRNA [68]. In addition, Kennedy et al. reported that m^{6}A addition at HIV-1 3'UTR enhances viral gene expression *via* a mechanism linked to cellular YTHDF proteins recruitment [29]. However, the exact molecular mechanism underlying HIV-1 RNA metabolism upon ALKBH5 inhibition remains to be elucidated.

Conclusions

Our study provides proof-of-concept that modulating the m^{6}A pathway, specifically *via* ALKBH5 inhibition, can significantly enhance romidepsin-mediated reactivation of latent HIV-1. Future studies should focus on identifying new derivatives of ALKi-3 or other inhibitors of ALKBH5 as more potent LRAs. Moreover, we did not explore the killing effects of immune cells upon latent viral reactivation by combined treatment of romidepsin with ALKi-3. This approach may represent a promising adjunct to existing latency-reversing protocols and provide a concept of "dual-kick" to target transcriptional and post-transcriptional steps to enhance viral reactivation from HIV-1 latency.

Abbreviations

ART	Antiretroviral therapy
LRAs	Latency reversal agents
HDAC	Histone deacetylase
DNMT	DNA methyltransferases
HMT	Histone methyltransferase
PKC	Protein kinase C
TLR	Toll like receptor
IC	Immune checkpoint
NF-κB	Nuclear factor kappa B
m^{6}A	N6-methyladenosine
PLWH	People living with HIV
ALKi-3	ALKBH5 inhibitor 3
MeRIP	m^{6}A methylated RNA immunoprecipitation
PA-m^{6}A-seq	Photo-crosslinking-assisted m^{6}A sequencing
RRE	Rev responsive element
CA-p24	Capsid p24
FISH	Fluorescence in situ hybridization
RNA-seq	RNA sequencing

Supplementary Information

The online version contains supplementary material available at https://doi.org/10.1186/s12985-025-02744-4.

Supplementary Material 1

Acknowledgements

We thank the HIV-1+ individuals for their willingness to participate in this study. We thank the nursing team of CHU St-Pierre, Université Libre de Bruxelles who cared for the HIV+ individuals. We thank Claire Thiry from the Transfusion Center of Charleroi (Belgium) for providing blood from healthy donors. We thank Marzena Lenart from the Department of Clinical Immunology of the Jagiellonian University Collegium Medicum (Poland) for providing elutriated lymphocytes from healthy donors. We thank IFOM for providing access to the server. A.K.-P. and H.A. acknowledges funding from the National Science Centre, Poland (Sonata BIS Grant UMO-2018/30/E/NZ1/00874). H.A. acknowledges funding from the National Science Centre, Poland (Preludium Grant UMO-2022/45/N/NZ6/04203). C.V.L. acknowledges funding from the Belgian National Fund for Scientific Research (F.R.S-FNRS, Belgium), the French INSERM agency "ANRS/Maladies infectieuses émergentes", ViiV Healthcare, the "Fondation Roi Baudouin", the Internationale Brachet Stiftung (IBS), The "Amis des Instituts Pasteur à Bruxelles, asbl", and the US National Institutes of Health (NIH) (MDC grant UM1AI164562 co-funded by National Heart, Lung and Blood Institute, National Institute of Diabetes and Digestive and Kidney Diseases, National Institute of Neurological Disorders and Stroke, National Institute on Drug Abuse and the National Institute of Allergy and Infectious Diseases). M.B. was funded by fellowships from the Belgian « Fonds pour la formation à la Recherche dans l'Industrie et dans l'Agriculture (FRIA) (F.R.S.-FNRS) » and then from "Les Amis des Instituts Pasteur à Bruxelles, asbl". A. Dutilleul was funded by an "Aspirant" fellowship from the

F.R.S.-FNRS, by a fellowship from the "Les Amis des Instituts Pasteur à Bruxelles, asbl", and then by a "PDR" grant (PDR 40021157) from the F.R.S-FNRS. C.V.L. is "Directrice de Recherches" of the F.R.S-FNRS. The laboratory of C.V.L. is part of the ULB-Cancer Research Centre (U-CRC) (Faculty of Medicine, ULB).

Author contributions
Lead the study: A.K-P. Conceptualization, planning and design of the experiments: A.K-P., C.V.L., A.O.P., H.A., J.W. and M.B. Supervision of the work: A.K-P., C.V.L. and A.O.P. Methodology, perform the experiments: A.K-P., H.A., J.W., M.B., A.D., L.N., K.L. Performed HIV+ individuals' selection: C.N., S.D.W. Software: H.C.C., P.M. Formal analysis: A.K-P., H.A., M.B., A.D., P.M., C.V.L., A.O.P. Investigation: A.K-P., H.A., C.V.L., A.O.P., V.A.F., A.M., C.N., S.D.W. Resources: A.K-P., H.A., S.S., E.K., M.K, C.V.L. Data curation: A.K-P., H.A. Writing of original draft manuscript: A.K-P. and H.A. Writing, manuscript review and editing: A.K-P., H.A., K.P., H.C.C., M.B., C.V.L., A.O.P. Visualization: A.K-P, H.A. Project administration: A.K-P., H.A., C.V.L. Funding acquisition: A.K-P., H.A, A.O.P., C.V.L. All authors read or provided comments on the manuscript. All data were validated by A.K-P, C.V.L., A.O.P.

Data availability
No datasets were generated or analysed during the current study.

Declarations

Ethics approval and consent to participate
Ethical approval was granted by the Human Subject Ethics Committees of the Saint-Pierre Hospital (Brussels, Belgium). All individuals enrolled in the study provided written informed consent for donating blood.

Consent for publication
Not applicable.

Conflict of interest
A.O.P. received a research grant from Gilead Sciences Research Program. C.V.L. received a research grant from ViiV Healthcare. The funders had no role in study design, data collection and analysis, decision to publish, or preparation of the manuscript. The other authors declare no competing interests.

Competing interests
The authors declare no competing interests.

Author details
[1]Laboratory of Molecular Virology, Malopolska Centre of Biotechnology, Jagiellonian University, Kraków, Poland
[2]Doctoral School of Exact and Natural Sciences, Jagiellonian University, Kraków, Poland
[3]Service of Molecular Virology, Department of Molecular Biology (DBM), Université Libre de Bruxelles (ULB), Gosselies, Belgium
[4]Quantitative Virology Research Group, Population Diagnostics Center, Lukasiewicz Research Network– PORT Polish Center for Technology Development, Wroclaw, Poland
[5]The Laboratory of Quantitative Virology, Centre for Advanced Materials and Technologies, Warsaw University of Technology, 19 Poleczki St, Warsaw 02-822, Poland
[6]Dept of Molecular Medicine and Medical Biotechnology, Università degli Studi di Napoli "Federico II", Naples, Italy
[7]Institute of Chemistry, University of Tartu, Tartu, Estonia
[8]Université Paris Cité, INSERM U1016, CNRS UMR8104, Institut Cochin, Paris, France
[9]CHU d'Orléans, Orléans, France
[10]Service des Maladies Infectieuses, CHU St-Pierre, Université Libre de Bruxelles (ULB), Brussels 1000, Belgium
[11]Laboratory of Molecular Virology, The International Centre of Genetic Engineering and Biotechnology, Trieste, Italy
[12]Department of Pharmacology, Faculty of Medicine, University of Helsinki, Helsinki 00014, Finland
[13]Virogenetics Laboratory of Virology, Malopolska Centre of Biotechnology, Jagiellonian University, Kraków, Poland
[14]Laboratory of Experimental Virology, Department of Medical Microbiology, Amsterdam UMC, University of Amsterdam, Amsterdam, Netherlands

Received: 4 November 2024 / Accepted: 15 April 2025
Published online: 28 April 2025

References

1. Deeks SG, Lewin SR, Havlir DV. The end of AIDS: HIV infection as a chronic disease. Lancet. 2013;382:1525–33.
2. McMyn NF, Varriale J, Fray EJ, Zitzmann C, MacLeod H, Lai J, Singhal A, Moskovljevic M, Garcia MA, Lopez BM, Hariharan V, Rhodehouse K, Lynn K, Tebas P, Mounzer K, Montaner LJ, Benko E, Kovacs C, Hoh R, Simonetti FR, Laird GM, Deeks SG, Ribeiro RM, Perelson AS, Siliciano RF, Siliciano JM. The latent reservoir of inducible, infectious HIV-1 does not decrease despite decades of antiretroviral therapy. J Clin Invest. 2023;133:e171554.
3. Siliciano JD, Kajdas J, Finzi D, Quinn TC, Chadwick K, Margolick JB, Kovacs C, Gange SJ, Siliciano RF. Long-term follow-up studies confirm the stability of the latent reservoir for HIV-1 in resting CD4 + T cells. Nat Med. 2003;9:727–8.
4. Wong JK, Hezareh M, Günthard HF, Havlir DV, Ignacio CC, Spina CA, Richman DD. Recovery of Replication-Competent HIV despite prolonged suppression of plasma viremia. Science. 1997;278:1291–5.
5. Sadowski I, Hashemi FB. Strategies to eradicate HIV from infected patients: elimination of latent provirus reservoirs. Cell Mol Life Sci. 2019;76:3583–600.
6. Sengupta S, Siliciano RF. Targeting the latent reservoir for HIV-1. Immunity. 2018;48:872–95.
7. Ait-Ammar A, Kula A, Darcis G, Verdikt R, De Wit S, Gautier V, Mallon PWG, Marcello A, Rohr O, Van Lint C. Current status of latency reversing agents facing the heterogeneity of HIV-1 cellular and tissue reservoirs. Front Microbiol. 2020;10:3060.
8. Grau-Expósito J, Luque-Ballesteros L, Navarro J, Curran A, Burgos J, Ribera E, Torrella A, Planas B, Badía R, Martin-Castillo M, Fernández-Sojo J, Genescà M, Falcó V, Buzon MJ. Latency reversal agents affect differently the latent reservoir present in distinct CD4 + T subpopulations. PLOS Pathog. 2019;15:e1007991.
9. Kula-Pacurar A, Rodari A, Darcis G, Van Lint C. Shocking HIV-1 with Immunomodulatory latency reversing agents. Semin Immunol. 2021;51:101478.
10. Archin NM, Liberty AL, Kashuba AD, Choudhary SK, Kuruc JD, Crooks AM, Parker DC, Anderson EM, Kearney MF, Strain MC, Richman DD, Hudgens MG, Bosch RJ, Coffin JM, Eron JJ, Hazuda DJ, Margolis DM. Administration of Vorinostat disrupts HIV-1 latency in patients on antiretroviral therapy. Nature. 2012;487:482–5.
11. Moron-Lopez S, Kim P, Søgaard OS, Tolstrup M, Wong JK, Yukl SA. Characterization of the HIV-1 transcription profile after Romidepsin administration in ART-suppressed individuals. AIDS. 2019;33:425–31.
12. Rasmussen TA, Tolstrup M, Brinkmann CR, Olesen R, Erikstrup C, Solomon A, Winckelmann A, Palmer S, Dinarello C, Buzon M, Lichterfeld M, Lewin SR, Østergaard L, Søgaard OS. Panobinostat, a histone deacetylase inhibitor, for latent-virus reactivation in HIV-infected patients on suppressive antiretroviral therapy: a phase 1/2, single group, clinical trial. Lancet HIV. 2014;1:e13–21.
13. Gutiérrez C, Serrano-Villar S, Madrid-Elena N, Pérez-Elías MJ, Martín ME, Barbas C, Ruipérez J, Muñoz E, Muñoz-Fernández MA, Castor T, Moreno S. Bryostatin-1 for latent virus reactivation in HIV-infected patients on antiretroviral therapy. AIDS. 2016;30:1385–92.
14. Bullen CK, Laird GM, Durand CM, Siliciano JD, Siliciano RF. New ex vivo approaches distinguish effective and ineffective single agents for reversing HIV-1 latency in vivo. Nat Med. 2014;20:425–9.
15. Board NL, Yuan Z, Wu F, Moskovljevic M, Ravi M, Sengupta S, Mun SS, Simonetti FR, Lai J, Tebas P, Lynn K, Hoh R, Deeks SG, Siliciano JD, Montaner LJ, Siliciano RF. Bispecific antibodies promote natural killer cell-mediated elimination of HIV-1 reservoir cells. Nat Immunol. 2024;25:462–70.
16. Darcis G, Kula A, Bouchat S, Fujinaga K, Corazza F, Ait-Ammar A, Delacourt N, Melard A, Kabeya K, Vanhulle C, Van Driessche B, Gatot J-S, Cherrier T, Pianowski LF, Gama L, Schwartz C, Vila J, Burny A, Clumeck N, Moutschen M, De Wit S, Peterlin BM, Rouzioux C, Rohr O, Van Lint C. An in-Depth comparison of latency-Reversing agent combinations in various in vitro and ex vivo HIV-1 latency models identified Bryostatin-1 + JQ1 and ingenol-B + JQ1 to potently reactivate viral gene expression. PLoS Pathog. 2015;11:e1005063.
17. Laird GM, Bullen CK, Rosenbloom DIS, Martin AR, Hill AL, Durand CM, Siliciano JD, Siliciano RF. Ex vivo analysis identifies effective HIV-1 latency–reversing drug combinations. J Clin Invest. 2015;125:1901–12.
18. Bouchat S, Delacourt N, Kula A, Darcis G, Van Driessche B, Corazza F, Gatot J, Melard A, Vanhulle C, Kabeya K, Pardons M, Avettand-Fenoel V, Clumeck N, De Wit S, Rohr O, Rouzioux C. Lint, C. Sequential treatment with

5-aza-2′-deoxycytidine and deacetylase inhibitors reactivates HIV-1. EMBO Mol Med. 2016;8:117–38. Van.
19. Mohammadi P, di Iulio J, Muñoz M, Martinez R, Bartha I, Cavassini M, Thorball C, Fellay J, Beerenwinkel N, Ciuffi A, Telenti A. Dynamics of HIV latency and reactivation in a primary CD4 + T cell model. PLoS Pathog. 2014;10:e1004156.
20. Dorman A, Bendoumou M, Valaitiene A, Wadas J, Ali H, Dutilleul A, Maiuri P, Nestola L, Bociaga-Jasik M, Mchantaf G, Avettand-Fenoël V, Marcello A, Pyrc K, Pasternak AO, Lint CV. Kula-Pacurar, A. PP1.1–00164 nuclear retention of unspliced HIV-1 RNA as a novel reversible posttranscriptional block in latency. J Virus Erad. 2024;10:39.
21. Zaccara S, Ries RJ, Jaffrey SR. Reading, writing and erasing mRNA methylation. Nat Rev Mol Cell Biol. 2019;20:608–24.
22. Dong S, Wu Y, Liu Y, Weng H, Huang H. N6 -methyladenosine steers RNA metabolism and regulation in Cancer. Cancer Commun Lond Engl. 2021;41:538–59.
23. Shi H, Wei J, He C. Where, when, and how: Context-Dependent functions of RNA methylation writers, readers, and erasers. Mol Cell. 2019;74:640–50.
24. Luo Q, Gao Y, Zhang L, Rao J, Guo Y, Huang Z, Li J, Decreased. *ALKBH5*, *FTO*, and *YTHDF2* in Peripheral Blood Are as Risk Factors for Rheumatoid Arthritis. *BioMed Res. Int.* 2020, 5735279 (2020).
25. Qu J, Yan H, Hou Y, Cao W, Liu Y, Zhang E, He J, Cai. Z. RNA demethylase ALKBH5 in cancer: from mechanisms to therapeutic potential. J Hematol Oncol J Hematol Oncol. 2022;15:8.
26. Wei C, Wang B, Peng D, Zhang X, Li Z, Luo L, He Y, Liang H, Du X, Li S, Zhang S, Zhang Z, Han L, Zhang J. Pan-Cancer analysis shows that ALKBH5 is a potential prognostic and immunotherapeutic biomarker for multiple Cancer types including gliomas. Front Immunol. 2022;13:849592.
27. Jiang X, Liu B, Nie Z, Duan L, Xiong Q, Jin Z, Yang C, Chen Y. The role of m6A modification in the biological functions and diseases. Signal Transduct Target Ther. 2021;6:74.
28. Lichinchi G, Gao S, Saletore Y, Gonzalez GM, Bansal V, Wang Y, Mason CE, Rana TM. Dynamics of the human and viral m(6)A RNA methylomes during HIV-1 infection of T cells. Nat Microbiol. 2016;1:16011.
29. Kennedy EM, Bogerd HP, Kornepati AVR, Kang D, Ghoshal D, Marshall JB, Poling BC, Tsai K, Gokhale NS, Horner SM, Cullen BR. Posttranscriptional m(6) A editing of HIV-1 mRNAs enhances viral gene expression. Cell Host Microbe. 2016;19:675–85.
30. Cristinelli S, Angelino P, Janowczyk A, Delorenzi M, Ciuffi. A. HIV modifies the m6A and m5C epitranscriptomic landscape of the host cell. Front Virol. 2021;1:11.
31. Tsai K, Bogerd HP, Kennedy EM, Emery A, Swanstrom R, Cullen BR. Epitranscriptomic addition of m ^{6} A regulates HIV-1 RNA stability and alternative splicing. Genes Dev. 2021;35:992–1004.
32. N'Da Konan S, Ségéral E, Bejjani F, Bendoumou M, Ait Said M, Gallois-Montbrun S, Emiliani S. YTHDC1 regulates distinct post-integration steps of HIV-1 replication and is important for viral infectivity. Retrovirology. 2022;19:4.
33. Tirumuru N, Zhao BS, Lu W, Lu Z, He C, Wu L. N6-methyladenosine of HIV-1 RNA regulates viral infection and HIV-1 gag protein expression. eLife. 2016;5:e15528.
34. Lu W, Tirumuru N, Gelais S, Koneru C, Liu PC, Kvaratskhelia C, He M, C., Wu L. N6-Methyladenosine-binding proteins suppress HIV-1 infectivity and viral production. J Biol Chem. 2018;293:12992–3005.
35. Jurczyszak D, Zhang W, Terry SN, Kehrer T, Bermúdez González MC, McGregor E, Mulder LCF, Eckwahl MJ, Pan T. Simon, V. HIV protease cleaves the antiviral m6A reader protein YTHDF3 in the viral particle. PLoS Pathog. 2020;16:e1008305.
36. Selberg S, Žusinaite E, Herodes K, Seli N, Kankuri E, Merits A, Karelson M. HIV replication is increased by RNA methylation METTL3/METTL14/WTAP complex activators. ACS Omega. 2021;6:15957–63.
37. Selberg S, Seli N, Kankuri E, Karelson M. Rational design of novel anticancer Small-Molecule RNA m6A demethylase ALKBH5 inhibitors. ACS Omega. 2021;6:13310–20.
38. Yankova E, Blackaby W, Albertella M, Rak J, De Braekeleer E, Tsagkogeorga G, Pilka ES, Aspris D, Leggate D, Hendrick AG, Webster NA, Andrews B, Fosbeary R, Guest P, Irigoyen N, Eleftheriou M, Gozdecka M, Dias JML, Bannister AJ, Vick B, Jeremias I, Vassiliou GS, Rausch O, Tzelepis K, Kouzarides T. Small-molecule Inhibition of METTL3 as a strategy against myeloid leukaemia. Nature. 2021;593:597–601.
39. Liu L, Zhao T, Zheng S, Tang D, Han H, Yang C, Zheng X, Wang J, Ma J, Wei W, Wang Z, He S, He Q. METTL3 inhibitor STM2457 impairs tumor progression and enhances sensitivity to anlotinib in OSCC. Oral Dis. 2024;30:4243–54.
40. Ofir-Rosenfeld Y, Vasiliauskaitė L, Saunders C, Sapetschnig A, Tsagkogeorga G, Albertella M, Carkill M, Self-Fordham J, Holz JB, Rausch O. STC-15, an oral small molecule inhibitor of the RNA methyltransferase METTL3, inhibits tumour growth through activation of anti-cancer immune responses associated with increased interferon signalling, and synergises with T cell checkpoint Blockade. Eur J Cancer. 2022;174:123.
41. Bader JP, Brown NR, Chiang PK, Cantoni GL. 3-Deazaadenosine, an inhibitor of adenosylhomocysteine hydrolase, inhibits reproduction of Rous sarcoma virus and transformation of chick embryo cells. Virology. 1978;89:494–505.
42. Fischer AAH, Müller K, Scholtissek C. Specific Inhibition of the synthesis of influenza virus late proteins and stimulation of early, M2, and NS2 protein synthesis by 3-deazaadenosine. Virology. 1990;177:523–31.
43. Flexner CW, Hildreth JE, Kuncl RW, Drachman. DanielB. 3-deaza-adenosine and Inhibition of HIV. Lancet. 1992;339:438.
44. Selberg S, Blokhina D, Aatonen M, Koivisto P, Siltanen A, Mervaala E, Kankuri E, Karelson M. Discovery of small molecules that activate RNA methylation through cooperative binding to the METTL3-14-WTAP complex active site. Cell Rep. 2019;26:3762–e37715.
45. Jordan A. HIV reproducibly establishes a latent infection after acute infection of T cells in vitro. EMBO J. 2003;22:1868–77.
46. Folks TM, Justement J, Kinter A, Dinarello CA, Fauci AS. Cytokine-Induced expression of HIV-1 in a chronically infected promonocyte cell line. Science. 1987;238:800–2.
47. Dorman A, Bendoumou M, Valaitienė A, Wadas J, Ali H, Dutilleul A, Maiuri P, Nestola L, Bociaga-Jasik M, Mchantaf G, Necsoi C, De Wit S, Avettand-Fenoël V, Marcello A, Pyrc K, Pasternak AO, Van Lint C. Kula-Pacurar, A. Nuclear retention of unspliced HIV-1 RNA as a reversible post-transcriptional block in latency. Nat Commun. 2025;16:2078.
48. Linkert M, Rueden CT, Allan C, Burel J-M, Moore W, Patterson A, Loranger B, Moore J, Neves C, MacDonald D, Tarkowska A, Sticco C, Hill E, Rossner M, Eliceiri KW, Swedlow JR. Metadata matters: access to image data in the real world. J Cell Biol. 2010;189:777–82.
49. Bolte S, Cordelières FP. A guided tour into subcellular colocalization analysis in light microscopy. J Microsc. 2006;224:213–32.
50. Selberg S, Yu L-Y, Bondarenko O, Kankuri E, Seli N, Kovaleva V, Herodes K, Saarma M, Karelson M. Small-Molecule inhibitors of the RNA M6A demethylases FTO potently support the survival of dopamine neurons. Int J Mol Sci. 2021;22:4537.
51. Yukl SA, Kaiser P, Kim P, Telwatte S, Joshi SK, Vu M, Lampiris H, Wong J. K. HIV latency in isolated patient CD4 + T cells May be due to blocks in HIV transcriptional elongation, completion, and splicing. Sci Transl Med. 2018;10:eaap9927.
52. Telwatte S, Lee S, Somsouk M, Hatano H, Baker C, Kaiser P, Kim P, Chen T-H, Milush J, Hunt PW, Deeks SG, Wong JK, Yukl SA. Gut and blood differ in constitutive blocks to HIV transcription, suggesting tissue-specific differences in the mechanisms that govern HIV latency. PLoS Pathog. 2018;14:e1007357.
53. Lassen KG, Ramyar KX, Bailey JR, Zhou Y, Siliciano RF. Nuclear retention of multiply spliced HIV-1 RNA in resting CD4 + T cells. PLoS Pathog. 2006;2:e68.
54. Bertino EM, Otterson GA. Romidepsin: a novel histone deacetylase inhibitor for cancer. Expert Opin Investig Drugs. 2011;20:1151–8.
55. Wei DG, Chiang V, Fyne E, Balakrishnan M, Barnes T, Graupe M, Hesselgesser J, Irrinki A, Murry JP, Stepan G, Stray KM, Tsai A, Yu H, Spindler J, Kearney M, Spina CA, McMahon D, Lalezari J, Sloan D, Mellors J, Geleziunas R, Cihlar T. Histone deacetylase inhibitor Romidepsin induces HIV expression in CD4 T cells from patients on suppressive antiretroviral therapy at concentrations achieved by clinical dosing. PLoS Pathog. 2014;10:e1004071.
56. Søgaard OS, Graversen ME, Leth S, Olesen R, Brinkmann CR, Nissen SK, Kjaer AS, Schleimann MH, Denton PW, Hey-Cunningham WJ, Koelsch KK, Pantaleo G, Krogsgaard K, Sommerfelt M, Fromentin R, Chomont N, Rasmussen TA, Østergaard L, Tolstrup M. The depsipeptide Romidepsin reverses HIV-1 latency in vivo. PLOS Pathog. 2015;11:e1005142.
57. Gunst JD, Pahus MH, Rosás-Umbert M, Lu I-N, Benfield T, Nielsen H, Johansen IS, Mohey R, Østergaard L, Klastrup V, Khan M, Schleimann MH, Olesen R, Støvring H, Denton PW, Kinloch NN, Copertino DC, Ward AR, Alberto WDC, Nielsen SD, Puertas MC, Ramos V, Reeves JD, Petropoulos CJ, Martinez-Picado J, Brumme ZL, Jones RB, Fox J, Tolstrup M, Nussenzweig MC, Caskey M, Fidler S, Søgaard OS. Early intervention with 3BNC117 and Romidepsin at antiretroviral treatment initiation in people with HIV-1: a phase 1b/2a, randomized trial. Nat Med. 2022;28:2424–35.
58. Leth S, Schleimann MH, Nissen SK, Højen JF, Olesen R, Graversen ME, Jørgensen S, Kjær AS, Denton PW, Mørk A, Sommerfelt MA, Krogsgaard K, Østergaard L, Rasmussen TA, Tolstrup M, Søgaard OS. Combined effect of

Vacc-4x, Recombinant human granulocyte macrophage colony-stimulating factor vaccination, and Romidepsin on the HIV-1 reservoir (REDUC): a single-arm, phase 1B/2A trial. Lancet HIV. 2016;3:e463–72.
59. Mishra T, Phillips S, Zhao Y, Wilms B, He C, Wu L. Epitranscriptomic m^6 A modifications during reactivation of HIV-1 latency in $CD4^+$ T cells. mBio. 2024;15:e02214–24.
60. Zhao M, De Crignis E, Rokx C, Verbon A, Gelder TV, Mahmoudi T, et la. T cell toxicity of HIV latency reversing agents. Pharmacol Res 2019;139:524–34. https://doi.org/10.1016/j.phrs.2018.10.023
61. Deng Q, Guo T, Qiu Z, Chen Y. Modeling the cytotoxicity of Romidepsin reveals the ineffectiveness of this drug in the "shock and kill" strategy 2023;173:113702. https://doi.org/10.1016/j.chaos.2023.113702
62. Kula A, Delacourt N, Bouchat S, Darcis G, Avettand-Fenoel V, Verdikt R, Corazza F, Necsoi C, Vanhulle C, Bendoumou M, Burny A, De Wit S, Rouzioux C, Rohr O, Van Lint C. Heterogeneous HIV-1 reactivation patterns of Disulfiram and combined Disulfiram + Romidepsin treatments. J Acquir Immune Defic Syndr 1999. 2019;80:605–13.
63. Tegowski M, Flamand MN, Meyer K. D. scDART-seq reveals distinct m6A signatures and mRNA methylation heterogeneity in single cells. Mol Cell. 2022;82:868–e87810.
64. McIntyre W, Netzband R, Bonenfant G, Biegel JM, Miller C, Fuchs G, Henderson E, Arra M, Canki M, Fabris D, Pager CT. Positive-sense RNA viruses reveal the complexity and dynamics of the cellular and viral epitranscriptomes during infection. Nucleic Acids Res. 2018;46:5776–91.
65. Pereira-Montecinos C, Toro-Ascuy D, Ananías-Sáez C, Gaete-Argel A, Rojas-Fuentes C, Riquelme-Barrios S, Rojas-Araya B, García-de-Gracia F, Aguilera-Cortés P, Chnaiderman J, Acevedo ML, Valiente-Echeverría F, Soto-Rifo R. Epitranscriptomic regulation of HIV-1 full-length RNA packaging. Nucleic Acids Res. 2022;50:2302–18.
66. Courtney DG, Tsai K, Bogerd HP, Kennedy EM, Law BA, Emery A, Swanstrom R, Holley CL, Cullen BR. Epitranscriptomic addition of m5C to HIV-1 transcripts regulates viral gene expression. Cell Host Microbe. 2019;26:217–e2276.
67. Baek A, Lee G-E, Golconda S, Rayhan A, Manganaris AA, Chen S, Tirumuru N, Yu H, Kim S, Kimmel C, Zablocki O, Sullivan MB, Addepalli B, Wu L, Kim S. Single-molecule epitranscriptomic analysis of full-length HIV-1 RNAs reveals functional roles of site-specific m6As. Nat Microbiol. 2024;9:1340–55.
68. Wang X, Lu Z, Gomez A, Hon GC, Yue Y, Han D, Fu Y, Parisien M, Dai Q, Jia G, Ren B, Pan T, He C. N6-methyladenosine-dependent regulation of messenger RNA stability. Nature. 2014;505:117–20.

Publisher's note